Article:
Figueredo, LFC, Castro Aguiar, R, Chen, L et al. (3 more authors) (2021) Human Comfortability: Integrating Ergonomics and Muscular-Informed Metrics for Manipulability Analysis During Human-Robot Collaboration. IEEE Robotics and Automation Letters, 6 (2). pp. 351-358. ISSN 2377-3766

https://doi.org/10.1109/LRA.2020.3043173

Human Comfortability: Integrating Ergonomics and Muscular-Informed Metrics for Manipulability Analysis during Human-Robot Collaboration

Luis F. C. Figueredo, Rafael Castro Aguiar, Lipeng Chen, Samit Chakrabarty,
Mehmet R. Dogar, Anthony G. Cohn

***Abstract*—The ability to compute a quality index for manipulation tasks, in different configurations, has been widely used in robotics. However, it is poorly explored in human manipulation and physical human-robot collaboration (pHRC). Existing works that evaluate efficiency of human manipulation often focus only on heurisitic-based, biomechanics or ergonomics methods/tasks. Complementarity between these performance features allows for a better evaluation and more general criteria, applicable across tasks. This paper addressess this gap by generating a new metric that combines offline pre-computation of biomechanics, ergonomics, muscle assessment and joint constraints, and reducing the online time complexity, enhancing the response query time. The proposed solution allow us to build a quality distribution in the human's workspace which can be quickly tailored to specific tasks and filtered for design purposes. This method simplifies human manipulability assessment for both general and task-specific applications and, in contrast to existing works, is suitable for real-time and/or resource-limited applications. Numerical evidence shows the proposed analysis greatly outperforms previous results in terms of computing time without compromising performance.**

***Index Terms*—Human-Centered Robotics; Human Factors and Human-in-the-Loop; Physical Human-Robot Interaction**

I. Introduction

Recent advances in robotics technologies are closing the gap between humans and robots. Nonetheless, robots are still rarely thought of being physically engaging with humans and efficient physical human-robot collaboration (pHRC) is one of the key open challenges in robotics research. When autonomously interacting with humans, robots need better decision-making capabilities which are hindered by the lack of a reliable quantitative assessment of human modeling and behavior [1]. Particularly in collaborative manipulation, the understanding of human physical capabilities and ergonomics is a cornerstone to any intelligent system that aims to either predict/analyze human movement or to leverage human's response to physical collaborative actions. For instance, consider the pHRC in Figs. 1-2 where a robot positions a board for the human to apply a task-specific force. The robot chooses the pose to optimize human comfort [2], [3]. In this context, increasing attention has been given to the control and planning of robot actions based on either *biomechanics aspects* (in terms of muscular activity) or *ergonomics* (in terms of industrial-standard postural assessment).

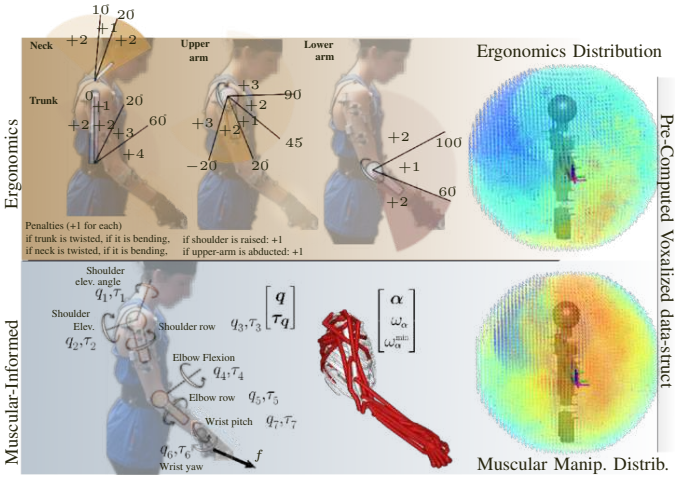

Figure 1: Outline for precomputed comfort assessment drawing on muscle-activity effort and posture scores. High/low comfortability points are shown in red/blue colors.

In recent years, a new thrust of robotics research has looked into biomechanics knowledge to produce insights into human motion synthesis mechanisms [4], [5]. In particular, muscular-informed metrics combined with improved simulation tools [6] and elaborated musculoskeletal models [7] have formed the basis of novel studies leveraging task-space-oriented approaches to movement sequence reconstruction and muscular-informed pHRC. Indeed, predicting muscular performance based on dynamics and task forces is crucial to extend the field of robotics to address the challenges involved in elaborate and fluid pHRC. In this context, Peternel et al. [3], [8] have presented excellent results focusing on muscular-activity-based fatigue

Manuscript received: July 1, 2020; Revised: October 6, 2020; Accepted: November 6, 2020.

This paper was recommended for publication by Editor Tamim Asfour upon evaluation of the Associate Editor and Reviewers' comments. This work was supported by the EU Horizon 2020 programme under the Marie Sklodowska-Curie grant No 795714, the AI4EU project (No 825619).

Luis F. C. Figueredo is with the Munich School of Robotics and Machine Intelligence, MSRM, Technical University of Munich, 80797, Germany. He is also a Visiting Research Fellow in the School of Computing, Faculty of Engineering and Physical Sciences, University of Leeds, LS2 9JT, UK. Email: figueredo@ieee.org.

Lipeng Chen, Mehmet R. Dogar and Anthony G. Cohn are with the School of Computing, Faculty of Engineering and Physical Sciences, University of Leeds, LS2 9JT, UK. A.G. Cohn is partially supported by the Alan Turing Institute and holds visiting positions at Luzhong Institute of Safety, Environmental Protection Engeering & Materials, Qingdao University of Science & Technology, Shandong University and Tongji University. Email: {sclc, m.r.dogar, a.g.Cohn}@leeds.ac.uk.

Rafael Castro Aguiar and Samit Chakrabarty are with School of Biomedical Sciences, Faculty of Biological Sciences, University of Leeds, UK. Email: {bsrdca, s.chakrabarty}@leeds.ac.uk

Digital Object Identifier (DOI): see top of this page.

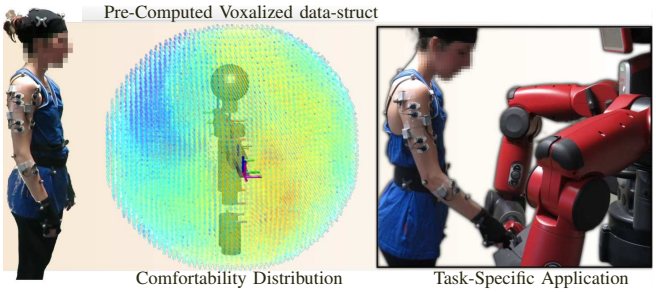

Figure 2: Combined muscular-based and ergonomy-based distribution applied to a pHRC puncturing task.

estimation and adaptation through robot-tool attitude control. Using similar muscular-activity assessment, our previous work [2] presented an optimization-based pHRC planner that uses human muscle-space to decide on a robot grasp and object positioning that maximizes muscular comfort (and peripersonal space). One major drawback of such methods, emphasized in [2], is the computation time required to explore the task-to-muscle-space redundant mapping and the task-space itself, i.e., the freedom of where to position the shared object.

In contrast to muscular-informed methods, standard ergonomics concepts like RULA (rapid upper limb assessment, see [9]) and REBA (rapid entire body assessment, see [10]) were designed to quickly and easily assess human posture and have been used in industrial scenarios for decades. Recently, these methods have also been extended to different robotics applications, e.g., task-planning [11].

Muscular-activity-based and ergonomy-based metrics both have strengths and limitations. Ergonomic concepts are well-posed for high-level rapid task-planning, yet they fail to address the impact and magnitude of larger forces and dynamic constraints in pHRC, which are better captured through muscular-based performance metrics. Muscular-informed metrics, on the other hand, fail to address the influence of static postural factors, repeatability of actions, experts' experience (embodied in ergonomic methods) but, most importantly, they have not been tested in industrial applications. Overall, there is a clear trade-off between ergonomic and muscular-informed metrics, but surprisingly there are no studies that investigate both methods. The existing literature employs either ergonomics or muscle activity metrics depending on the required task.

Contributions: In this paper, integrated ergonomic and muscular-informed manipulability metrics are given for the first time. To this aim, we adopt an approach fundamentally different from existing pHRC literature by building a human-specific manipulability data structure covering their workspace. The proposed approach takes robotics concepts of reachability [12] and manipulability distribution—which build on voxelized 3D or 6D grids with velocity/force manipulability index [13]—and extends them to muscular-based and ergonomics metrics. The outline strategy for individual metrics and to build a metric-specific manipulability distribution is shown in Fig. 1. This allows us to independently capture muscular-activity effort (required to either accelerate or produce task-forces) and postural ergonomics, integrating both in real-time, according to design objectives as shown in Fig. 2. This novel resulting metric is hereby termed a comfortability index.

Combining ergonomics and muscular-activity response to different conditions in terms of comfortability enables the designer to quickly filter performance for a given task condition. The precomputed data structure considerably simplifies assessment for both general and task-specific applications and, in contrast to existing works, is suitable for real-time and/or resource-limited applications. It is also extended to include self-collision information shaping the resulting distribution. Redundancy is also implicitly captured.

An additional contribution is the muscular-activity analysis, which follows a task-to-muscle-space optimization mapping that translates task-wrenches to muscular activity. In this work, we make use of the linearity of this map, only in terms of magnitude to build a data structure of muscular-informed manipulability (MiM) within the workspace. The precomputed data enables MiM information to be quired two to three orders of magnitude faster than standard approaches.

Finally, an implicit contribution is to enrich musculoskeletal model-based methods applicability. These methods, though advantageous, are still not commonly employed in industry, in favor of typical ergonomic measures. Combining both strategies introduces MiM to industrial and pHRC domains—replacing fully ergonomics metrics to one that increasingly relies on muscular-activity as the designer acquires confidence in model-based methods.

These contributions are presented as follows: Section II presents existing concepts in the literature concerning muscle-activity effort and postural ergonomics. These are the cornerstones for muscular-informed manipulability and the ergonomics index introduced in Section III. Both metrics are integrated into the human comfortability index, in Section IV, which is used to build the comfortability distribution and the task-specific comfortability analysis. Section V reports simulations and pHRC experiment results used to validate the approach and to illustrate its effectiveness. Lastly, Section VI presents conclusions and future-plans.

II. Preliminaries: Human-Informed Performance Criteria

This section provides a model-based muscle-activity as well as ergonomics–based REBA. These concepts shape the backbone of the comfortability analysis and are crucial for autonomously reasoning over ergonomics and biomechanics.

A. Muscle-Activity Effort: Task- to Muscle-Space Mapping

To reason over human biomechanics, we begin by recalling that similar to a robot manipulator, human limbs can be represented by kinematic chains, as shown in Fig. 1 (bottom left). In this context, task-space wrenches, $\boldsymbol{f} \in \mathbb{R}^6$, can be locally mapped to joint-space torques, $\boldsymbol{\tau} \in \mathbb{R}^7$, through the geometric Jacobian $\boldsymbol{J}$, at configuration $\boldsymbol{q}$, that is,

$$\boldsymbol{\tau} = \boldsymbol{J}^T(\boldsymbol{q})\,\boldsymbol{f}, \tag{1}$$

The above expression, ubiquitous in robotics, describes the map from task- to joint-space variables. Nonetheless, actuation in human kinesiology occurs in the muscle-space where muscle-tendon forces are transmitted to joint-torques. The transmission

(which can be seen as a mapping) in turn depends on a musculoskeletal model that defines muscular parameters [14], such as length, moment-arm (to joints) and how activation levels are mapped to joint-torques, as follows

$$\boldsymbol{\Gamma}\left(\boldsymbol{q}\right)\boldsymbol{\zeta}=\boldsymbol{\tau}, \tag{2a}$$

$$\boldsymbol{F}_{\text{m}}\left(\boldsymbol{q}\right)\boldsymbol{\alpha}=\boldsymbol{\zeta}, \tag{2b}$$

where $\boldsymbol{\zeta}\in\mathbb{R}^{\eta}$ is the vector of exerted muscle-tendon forces for a η-muscles system, while $\boldsymbol{\Gamma}\in\mathbb{R}^{7\times\eta}$ is a matrix-transformation that locally maps muscle forces to joint torques. In other words, $\boldsymbol{\Gamma}$ acts as the muscle-space Jacobian where each $\gamma_{ij}\in\mathbb{R}$ element contained in $\boldsymbol{\Gamma}$ depicts the moment-arm between the i^{th} muscle and the j^{th} joint. Hence, the i^{th} muscle contributes to the torque generated at the j^{th} joint through the moment-arm about the joint, that is, $\tau_j=\sum_i^{\eta}\gamma_{ij}\zeta_{i,}$. $\boldsymbol{F}_{\text{m}}=\operatorname{diag}\left(f_{1,m}^{\max},\ldots,f_{\eta,m}^{\max}\right)\in\mathbb{R}^{\eta\times\eta}$ is a diagonal matrix of maximum isometric muscle forces which gives way to a normalized muscle-activity $\boldsymbol{\alpha}\in\mathbb{R}^{\eta}$,

$$\boldsymbol{\alpha}\in\mathbb{M}^{\eta},\ \text{with}\ \ \mathbb{M}=\{\alpha_i\in\mathbb{R}\,|\,0\leq\alpha_i\leq1\}. \tag{3}$$

The matrices $\boldsymbol{F}_{\text{m}}$ and $\boldsymbol{\Gamma}$ are posture dependent, which reflects human variability to generate joint torques at different configurations $\boldsymbol{q}$. They are defined in [7] with a η=50 muscle segments model. This highly redundant muscle-space leads to an indeterminacy, where an infinite number of solutions satisfy (2). Thus, to estimate $\boldsymbol{\alpha}$, we exploit the kinesiology observation that humans resolve this redundancy in a consistent and optimal manner [15]. Optimality, in this case, refers to minimizing energy expenditure in terms of (3), i.e.,

$$\begin{aligned}\hat{\boldsymbol{\alpha}}=\arg\min_{\boldsymbol{\alpha}\in\mathbb{M}^{\eta}}&\left\{\boldsymbol{\alpha}^{T}\boldsymbol{\alpha}\right\}\\ &s.t.\,\boldsymbol{\Gamma}\left(\boldsymbol{q}\right)\boldsymbol{F}_{\text{m}}\left(\boldsymbol{q}\right)\boldsymbol{\alpha}=\boldsymbol{J}^{T}\left(\boldsymbol{q}\right)\boldsymbol{f},\end{aligned} \tag{4}$$

In addition to exerted task-space forces, it is also interesting to characterize the dynamic effects of task-space accelerations. As noticed by [5], [16], from the dynamic model, $\boldsymbol{M}\left(\boldsymbol{q}\right)\ddot{\boldsymbol{q}}+\boldsymbol{c}\left(\boldsymbol{q},\dot{\boldsymbol{q}}\right)+\boldsymbol{g}\left(\boldsymbol{q}\right)=\boldsymbol{\tau}$ (where $\boldsymbol{c}$ and $\boldsymbol{g}$ are respectively the centrifugal and Coriolis, and gravity torques, and $\boldsymbol{M}$ is the inertia matrix), the second order approximation for acceleration is $\ddot{\boldsymbol{x}}\cong\boldsymbol{J}\left(\boldsymbol{q}\right)\ddot{\boldsymbol{q}}$. Hence, the task-space acceleration to joint-torques is given by $\boldsymbol{\tau}\propto\boldsymbol{M}\left(\boldsymbol{q}\right)\boldsymbol{J}^{+}\left(\boldsymbol{q}\right)\ddot{\boldsymbol{x}}$, where $\boldsymbol{J}^{+}$ is the pseudo-inverse matrix. Note $\boldsymbol{M}$ is positive and $\boldsymbol{J}^{+}$ has the same input and output singular vectors as $\boldsymbol{J}^{T}$, hence the influence of the accelerations will be similar to task-space forces in (1). That is, an acceleration or a task-space force applied in the same direction yields similar joint-torques in terms of positiveness, yet with different weights.

B. Ergonomic Measure: REBA

To capture ergonomics, this work relies on the rapid entire body assessment technique, namely REBA [10]. This postural analysis draws a quantitative measure for ergonomics from experiments and experts evaluation—ergonomists, physiotherapists, among others.

Ergonomics is quantified by a scoring system over two groups: trunk, neck and legs and a second for the upper and lower arms and wrists. A score is assigned to each body part according to a set of 144 possible posture combinations. The lower the better in terms of ergonomics. Fig. 1 illustrates possible scores for the neck, trunk and upper limb. Additional penalties are given due to large load/forces (first group) and awkward/unsafe grasp (second group). An overall score (from 1 to 12) is computed, and a final penalty is added w.r.t. demanding activities—these activities are static (a pose held for longer than 1 minute), repetitive (more than 4 repetitions per minute), and/or abrupt.

It is important to emphasize the complementarity of both assessments. While postural ergonomics fail to capture high impact and task-to-muscle-space force transmission, they successfully measure different aspects of comfort/ergonomics that are either neglected or hard to characterize through biomechanics alone. Indeed, REBA being an inherently heuristic method provides rougher estimates on biomechanical aspects in exchange for a more comprehensive estimation of different human aspects, such as neurophysiology and psychosomatic factors. For instance, biomechanics model alone fails to address human perceived comfort, preferences, or the influence of complex or repetitive actions to muscular comfort and their influence over central fatigue.[1] These features are embodied in postural ergonomic metrics from several health studies and experts' evaluation.

In a similar fashion, a biomechanics mapping from task-to-muscle-space leads to configurations with lower muscle-activity and yet they may not be ergonomic (for instance, extending one's arm close to singularity to resist a pushing action may lead to lower torques yet it is not ergonomic). Furthermore, REBA includes additional body parts which are hard to characterize in terms of muscular-activity due to many issues, e.g., dimensionality and elaborate correlation.

One of our novel contributions is to capture the benefits and trade-offs from both ergonomy-based and muscular-activity-based metrics.

III. Muscular and Ergonomic Manipulabilities

A. Muscular-Informed Manipulability Measure

In this subsection, we design a muscular-informed manipulability measure from the muscular transmission rate to task-forces. More specifically, from a quantitative assessment of the task-space force generation capability w.r.t. the muscle-tendon maximum forces from the biomechanical model. Such an analysis is similar to how manipulability maps the force capability for a robot manipulator w.r.t. its joint-torque limits. In robotics, this can be quickly computed from the manipulability ellipsoid—spanned by the singular vectors of the Jacobian. Manipulability measures are drawn from the ellipsoid volume [17], the transmission rate (magnitude) along axis [18], the minimum singular value [19], or the condition number between minimum and maximum transmission rates (see [19] for advantages and drawbacks of each). Yet, in contrast to robotics, human muscular-activation ((3)) is not defined over a vector-space and, thus, does not admit an SVD spanning nor a pre-image analysis over the unit-norm (since the space in (3) has no norm).

[1]Central nervous system (CNS) fatigue is a phenomenon associated with CNS (mainly brain and spinal cord) neurochemical response to prolonged or repetitive exercises and cannot be explained by peripheral factors (e.g., mechanical and cellular changes) that affect muscle function.

In this context, instead of mapping $\mathbb{M}^\eta \to \mathbb{R}^\eta$ to analyze the corresponding manipulability ellipsoid—which has little physical meaning in muscle-space (see Remark 1)—we evaluate the bounds on the maximum task-space force capabilities along predetermined directions identified by unitary $\{-1, 0, +1\}^3$ forces and torques in task-space. To compute these bounds, we take advantage of the linearity of (4) w.r.t. to task-space forces. In other words, by normalizing the task-force—i.e., $\boldsymbol{f} = \overline{\boldsymbol{f}}\omega_\alpha$ where $\left\|\overline{\boldsymbol{f}}\right\| = 1$ and $\omega_\alpha = \|\boldsymbol{f}\| \in \mathbb{R}_{\geq 0}$—we can analyze the muscular effort w.r.t. to a unitary vector in that direction, that is, given (2), we have

$$\boldsymbol{\Gamma}(\boldsymbol{q})\boldsymbol{F}_{\text{m}}(\boldsymbol{q})\boldsymbol{\alpha} = \boldsymbol{J}^T(\boldsymbol{q})\,\overline{\boldsymbol{f}}.$$

Hence, the maximum task-space force along the unitary direction $\overline{\boldsymbol{f}}$ is given by

$$\omega_\alpha \triangleq \frac{1}{\max\{\boldsymbol{\alpha}\}} \tag{5}$$

which physically corresponds to achieving one of the muscle-segments force limit. Hence, this is the muscle-space limitation to apply forces in the task-space direction $\overline{\boldsymbol{f}}$ at a given $\boldsymbol{q}$ configuration. And, ω_α is the resulting maximum task-force magnitude. The resulting measure $\omega_\alpha \in \mathbb{R}_{\geq 0}$, in this sense, acts as a **muscular-informed transmission rate (MiTR)** from muscle-space capabilities to task-space forces along $\overline{\boldsymbol{f}}$.

From (5), a muscle-informed manipulability feasibility region can therefore be defined over a vector $\boldsymbol{\omega}_\alpha$ of muscular-based transmission rates checked along a set of $n-$forces $\boldsymbol{\mathcal{F}} \in \mathbb{R}^{6\times n}$ as shown in Fig. 3. In this work, we define the **muscular-informed manipulability (MiM) index** as the least muscular-based force generation capability among the set of forces $\boldsymbol{\mathcal{F}}$, that is,

$$\omega_\alpha^{\min} \triangleq \min\{\boldsymbol{\omega}_\alpha\}. \tag{6}$$

This manipulability index works similarly to the singular value for robot manipulators [20], but signifies the worst MiTR in the direction most difficult to apply forces, i.e., the closeness to the muscular limit.

Remark 1. The optimization (4) defines a constraint norm for $\boldsymbol{\alpha}$ that satisfies the set definition (3). This ensures positiveness in contrast to an induced norm over $\mathbb{R}^\eta$ often used for performance characterization metrics, i.e., $E \triangleq \hat{\boldsymbol{\alpha}}^T\hat{\boldsymbol{\alpha}}$,

$$E = \boldsymbol{\tau}^T\left(\boldsymbol{\Gamma}\boldsymbol{F}_{\text{m}}^2\boldsymbol{\Gamma}^T\right)^{-1}\boldsymbol{\tau} = \boldsymbol{f}^T\boldsymbol{J}\left(\boldsymbol{\Gamma}\boldsymbol{F}_{\text{m}}^2\boldsymbol{\Gamma}^T\right)^{-1}\boldsymbol{J}^T\boldsymbol{f}. \tag{7}$$

This solution is ill-conditioned as it neglects $\boldsymbol{\alpha}$ positiveness, i.e., it assumes the possibility of negative activation of muscles, which is physiologically unfeasible. The manipulability ellipsoid or measures from (7) similarly do not reflect the biomechanics capabilities as shown in Fig. 3. Indeed, the resulting ellipsoid will always overestimate the actual biomechanics capabilities which may lead to undesired higher muscular load.

Normalized Muscular-Informed Manipulability

To make both muscular-informed and ergonomics measures compatible,[2] we analyze (5)-(6) w.r.t. the most positive point in the workspace. Hence, we refer to **muscular-informed transmission rate (MiTR)** and **muscular-informed manipulability (MiM)** as the normalized values

$$\underline{\omega_\alpha} \triangleq \frac{\omega_\alpha}{\max\{\Omega_\alpha\}}, \tag{8}$$

$$\underline{\omega_\alpha^{\min}} \triangleq \frac{\omega_\alpha^{\min}}{\max\{\Omega_\alpha^{\min}\}}. \tag{9}$$

where Ω_α and $\Omega_\alpha^{\min}$ are respectively the set of all ω_α and $\omega_\alpha^{\min}$ within the workspace. Hence, $\max\{\Omega_\alpha\}$ and $\max\{\Omega_\alpha^{\min}\}$ are the human specific maximum MiTR and MiM. Section IV-B demonstrates how to compute the sets Ω_α and $\Omega_\alpha^{\min}$.

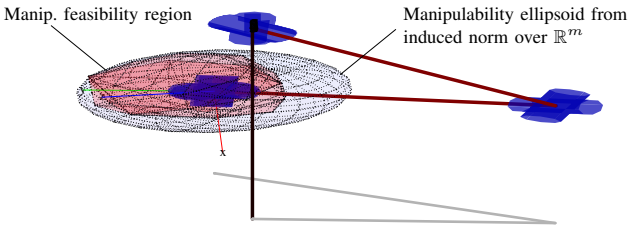

Figure 3: Comparison between task-space bounded 3D forces from biomechanics assessment (4)-(5) (red surface) with ellipsoid from the induced norm over $\mathbb{R}^m$ (7) (outer ellipsoid).

B. Ergonomics Quality Index

The REBA formulation outputs a stepwise linear score function ($r_e \in \mathbb{N}^+$) inversely proportional to ergonomic satisfaction from 1 (satisfactory working posture) to 15 (high risk of injury). Nonetheless, assessment of the REBA score is nonlinear in the terms of ergonomists' recommended actions [10], which are often divided into acceptable ($r_e=1$) or low-risk ($r_e=\{2,3\}$) postures which may or not require corrections, medium risk postures (often outside the ergonomic range of motion) if $r_e \in [4-7]$, and high ($r_e \in [8-10]$) and very high risk ($r_e \in [11-15]$) postures that require imminent or immediate corrections to reduce risk of injury. In this sense, an ergonomy-based index should not map REBA scores linearly. Take, for instance, a deviation of REBA from $\Delta r_e = 3$. From 10 to 13, there is little change in ergonomist assessment (unergonomic posture that should be fixed), whereas from $r_e = 1$ to 4 it indicates a major change in ergonomy condition (from satisfactory to a posture likely to be outside the ergonomic range of motion). To capture such experts' assessment, rather than a linear decreasing functional, we designed an ergonomic functional over a normalized REBA score, i.e., $\overline{r_e} \triangleq \frac{r_e-1}{\max(r_e)-1} \in [0,1]$, as

$$\omega_{\text{e}} \triangleq \left(1 + \overline{r_e}\cdot e^{\overline{r_e}}\right)^{-2}. \tag{10}$$

This leads to an **ergonomics index (ErI)** $\{\omega_{\text{e}} \in \mathbb{R} | \omega_{\text{e}} \in [0,1]\}$ which better addresses REBA significance. For instance, in the above example, a change from $r_e = 1$ to 4 produces a deviation of $\Delta\omega_{\text{e}} = 0.38$, while from $r_e = 10$ to 13 leads to ω_{e} varying from 0.20 to 0.11, i.e., $\Delta\omega_{\text{e}} = 0.09$.

C. Extended analysis: Collision Penalization

When addressing manipulability over the human workspace, self-collision plays an important part which is often neglected

[2]Notice that both metrics (5)-(6) are unbounded, that is, $\omega_\alpha, \omega_\alpha^{\min} \in \mathbb{R}_{\geq 0}$, which make them harder to scale with ergonomics conditions.

in the human-informed movement performance [5], [15] and control and planning [2], [11], [21] literature. Regardless of the muscular-to-force generation capability, our assumption is that humans restrain their actions when close to head or body. This closeness can be translated to penalties shaping the comfortability space.

The penalization is adapted from [13] based on the nearest points on the surface of the body part ($\boldsymbol{p}$) and the arm ($\boldsymbol{p}_h$). The distance from the human arm is hence defined by $d = \|\Delta\boldsymbol{p}\|$, where $\Delta\boldsymbol{p} = \boldsymbol{p} - \boldsymbol{p}_h$. A collision penalty function $\rho : \mathbb{R}^3 \to \mathbb{R}_{\geq 0}$ designed to modify the manipulability measure should $\rho \to 1$ if the arm is sufficiently away and goes to zero as $\boldsymbol{p}_h \to \boldsymbol{p}$. Adapting from [13, and 15 therein], we choose

$$\rho = \left(1 + e^{(-\sigma\Delta\boldsymbol{p})}\Delta\boldsymbol{p}^{-\varsigma}\right)^{-1}, \tag{11}$$

for which $\varsigma > 0$ satisfies a desired decay rate and $\sigma > 0$ is defined as $\sigma \triangleq -\frac{1}{d_d}\log\left(\frac{1-\rho_d}{\rho_d}d_d^{\varsigma}\right)$ with $\rho_d < 1$ being the desired penalty at a prescribed self-collision distance $d_d > 0$.[3] Now, depending on the body part, we are only interested in penalizing comfortability if exerted forces/accelerations have components deployed in their direction. Hence, the penalty function is rewritten as

$$\rho_s = \begin{cases} \rho, & \text{if } \boldsymbol{f}^T\Delta\bar{\boldsymbol{p}} > 0, \\ 1, & \text{otherwise,} \end{cases} \tag{12}$$

where $\Delta\bar{\boldsymbol{p}} \in \mathbb{R}^6$ is an augmented vector with a zero 3D vector to remove the influence of task-space torques—as collision avoidance is only applied to translation.

Obstacle Avoidance: In addition to self-collision, in the case where fixed obstacles are available in a scenario, e.g., a structured manufacturing plant, we can include obstacle avoidance penalties manipulability distributions. Obstacle penalization (ρ_o) can be assessed in a similar fashion to (12) and even included in the data structure construction. Additionally, obstacle penalization can also be included in a later step—as an update/reshaping of the comfortability map.

Notice that closeness to the desired object in a physical interaction context should not be penalized.

IV. Human Comfortability Analysis

A. Human Comfortability Index

Drawing from muscle-activity and ergonomic measures (9)-(10), a novel comfortability index is introduced following a framework similar to the compatibility index from Chiu [18] with additional penalization due to self-collision and obstacle avoidance, that is,

$$\varpi \triangleq \rho_o\rho_s\left(\kappa_\alpha\underline{\omega_\alpha^{\min}} + \kappa_{\mathrm{e}}\omega_{\mathrm{e}}\right). \tag{13}$$

Casting comfortability in terms of muscular-activity and ergonomics compatibility helps researchers evaluate human adaptability, optimize performance, and design collaborative robot actions. In this sense, the weights κ_α and κ_{e} are designed to capture the benefits and trade-offs from each performance index. For instance, giving more emphasis to ergonomics in repetitive light hand-over tasks while focusing on muscular-activity in case of a forceful interaction—for an example on how to design the gains, see Section V.

Notice the comfortability quality metric (13) implicitly considers human muscle- and joint-space redundancies since both $\underline{\omega_\alpha^{\min}}$ and ω_{e} penalize kinematic configurations leading to uncomfortable conditions and (4) optimizes over the biomechanics assumption of minimizing energy expenditure.

B. Human Comfortability Analysis

This section builds up a comfortability distribution in the workspace. The proposed approach, similar to robotics concepts of reachability and manipulability analysis [13], builds on a 3D or 6D voxelized data structure Ψ holding comfortability information in each voxel ψ.

A workspace representation and the resulting comfortability distribution are unique to individual's characteristics. The design involves scaling kinematics and musculoskeletal models to match a specific human's anthropometry features and provide user-specific kinematic and muscle-tendon (e.g., muscle-tendon lengths, moment arms, lines of action) parameters [7]. In this sense, comfortability accounts for differences between individuals features, as body sizes. While the influence in ergonomics is purely kinematic, muscular-based performance would result in slight differences in performance for the same task and joint-space configuration.

Given an individual's anthropometry features, the human comfort quality distribution in workspace can be designed in two different ways. Either task- or joint-space can be discretized and the resulting configurations analyzed to update the corresponding voxel ψ. In this work, the comfortability representation in workspace is built by randomly sampling a large set of joint-configurations. Each sample is thereafter analyzed in terms of its task-space pose by computing the forward kinematics model and categorized in the corresponding voxel ψ. Values for MiM and ErI are computed and stored. After analyzing all samples, we compute the set $\Omega_\alpha^{\min}$ of all $\omega_\alpha^{\min}$ values and add the normalized MiM measure $\underline{\omega_\alpha^{\min}}$ to each sample. Finally, we compute the resulting comfortability index ϖ from (13) given specific gains $\kappa_\alpha, \kappa_{\mathrm{e}}$ and penalties ρ_o and ρ_s. For each voxel, we select the configuration with higher comfortability index ϖ. This leads to an upper-bound representation of comfortability that resolves human kinematic redundancy in a consistent manner—optimizing comfortability—satisfying biomechanics assumption that redundancy acts to minimize the energy expenditure. This assumption, known as the kinematic minimum effort assumption, is extended herein to also address ergonomics and collision penalties. With this structure, penalties due to different obstacles can also be quickly updated and thereafter shape the comfortability index without having to reconstruct the dataset distribution.

C. Task-specific Comfortability Analysis

In many practical applications, we are instead interested in finding a task-specific comfortability index ($\mathcal{TS}$-comfortability), e.g., to analyze a pushing or throwing scenario. For applications where we know the acceleration

[3] In this work, we are considering different values for the head and trunk.

directions or forces involved, we can simplify the manipulability analysis from Subsection IV-B. In this case, comfortability information stored in each voxel ψ evaluates the muscular-informed transmission rate ω_α for the specific force $\boldsymbol{f}$ or acceleration direction—instead of the more general muscular-informed manipulability index $\omega_\alpha^{\min}$—together with the ergonomic index ω_{e}, as previously. From the resulting dataset, we compute the set Ω_α of all stored ω_α values and add the normalized MiTR $\underline{\omega_\alpha}$ to each sample. Finally, we compute the resulting task-specific comfortability index ϖ:

$$\varpi \triangleq \rho_o \rho_s \left(\kappa_\alpha \underline{\omega_\alpha} + \kappa_{\mathrm{e}} \omega_{\mathrm{e}}\right). \tag{14}$$

given specific gains $\kappa_\alpha, \kappa_{\mathrm{e}}$ and penalties ρ_o and ρ_s.

Fig. 4 presents one example of a human comfortability distribution and a $\mathcal{TS}$-comfortability considering a standard musculoskeletal model from [7] available in [6].

D. Task-specific Comfortability Implementation

To reduce the computational complexity of building a novel comfortability analysis for different task-specific applications, we propose a solution that explores an augmented comfortability analysis (designed offline) that can be quickly shaped towards a $\mathcal{TS}$-comfortability for a specific force $\boldsymbol{f}$ or acceleration. To this aim, instead of analyzing the MiM as in (6), the augmented comfortability analysis should store, at each voxel ψ, a vector $\boldsymbol{\omega}_\alpha$ of all muscular-based transmission rates along the set of $n-$forces $\boldsymbol{\mathcal{F}} \in \mathbb{R}^{6\times n}$.

Hence, we can compute for each voxel ψ an approximated MiTR for the task-specific force $\boldsymbol{f}$ through a weighted linear combination of the ι muscular-based transmission rates ω_α corresponding to the ι-closest forces—in terms of their scalar projection over $\boldsymbol{f}$. The projection angles themselves are used as weights for the linear combination of selected values in $\boldsymbol{\omega}_\alpha$ which produces the resulting MiTR $\underline{\omega_\alpha}$ for the task-specific force $\boldsymbol{f}$. Applying the same procedure for each voxel leads to an approximated task-specific comfortability assessment which can be computed as in (14).

The resulting $\mathcal{TS}$-comfortability has the same ergonomic features, yet slightly different muscular-based capabilities to (5). The $\mathcal{TS}$-comfortability can be used to quickly and efficiently approximate the expected comfortability of the specific pose in space w.r.t. to task-specific force. Conservativeness of this analysis is explored in Subsection V-A.

V. Applications and Quantitative Assessment

A. Muscular-informed quantitative assessment

This example analyzes the computational advantages and conservativeness of exploring a precomputed muscular-informed manipulability (MiM) datastructure in contrast to global optimizers (GOs). To this aim, we implemented 1000 different task-space forces and explored the capability of solvers based on GOs[4] (GO_1 and GO_2) without precomputation and MiM-based to find a configuration $\boldsymbol{q}$ that minimizes the muscular-activity effort $\|\boldsymbol{\alpha}\|$ for each force. This scenario was devised for a muscular-based planner in [2] to improve pHRC response, yet one of the main constraints of the method relates to its time-complexity. Herein, we analyze the efficiency of the $\mathcal{TS}$-comfortability implementation (Subsection IV-D with κ_α=1, κ_{e}=0) with the workspace voxelized into 10k datapoints—compared to GO_1 and GO_2.

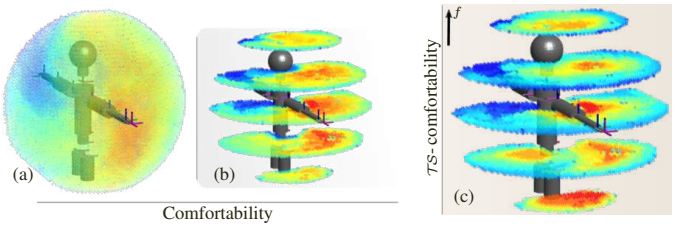

Figure 4: The 3D visualization of the 6D distribution considering κ_α=κ_{e}=0.5, and orientation with maximum comfortability per voxel, is shown in (a). In (b), we show different cuts through the distribution, similarly to (c) which shows the $\mathcal{TS}$-comfortability for a upwards task-force (e.g., lifting).

For each task-space force, we computed the optimal $\|\boldsymbol{\alpha}\|$ (and corresponding $\boldsymbol{q}$) from both GOs and from the ℓ-best results queried from MiM; i.e., we computed and selected the best $\|\boldsymbol{\alpha}\|$ from the ℓ queried joint-configurations. Results, in Table I, illustrate that MiM leads to solutions up to two-orders of magnitude faster, without compromising muscular performance.[5] The overall time includes the reshaping of datastruct which takes $0.033 \pm .003$. Results also show correlation between joint deviation and muscular effort.

	Muscle Act. Effort $\|\boldsymbol{\alpha}\|$ (a.u.)	Joint config. deviation (deg)	Overall Time (s)
GO_1	**1**	–	**42.5** $\pm$ 9.067
GO_2	**1.029** $\pm$ .159	**15.9** $\pm$ 10.3	**11.6** $\pm$ 1.894
MiM (ℓ_1)	**1.182** $\pm$ .265	**48.65** $\pm$ 24.2	**0.043** $\pm$ .003
MiM (ℓ_{30})	**1.109** $\pm$ .197	**23.4** $\pm$ 12.5	**0.804** $\pm$ .017

Table I: Muscular-informed manipulability (MiM) compared to global optimizers in terms of average execution time, joint deviation and activity effort normalized by GO_1.

B. Task Performance Evaluation

To further facilitate the design problem, we propose a simple methodology to capture task-requirements in terms of the benefits and trade-offs from muscular-informed and ergonomics indexes and compute weights κ_α and κ_{e}. For instance, a task involving larger forces/accelerations tend to be better captured by MiTR (higher κ_α), whereas slow execution and/or repetitive tasks with light loads are better captured through ergonomics. To aid the design problem, we compute the weights κ_α, κ_{e} as follows:

$$\begin{cases} \kappa_\alpha = \frac{1}{3}\left(\mathcal{T}_s + \mathcal{T}_i + (1 - \mathcal{T}_r)\right), \\ \kappa_{\mathrm{e}} = \left(1 - \kappa_\alpha\right), \end{cases}$$

where $\mathcal{T}_s \in \{0, 0.25, 0.5, 0.75, 1\}$ refers to the task-speed requirements—from steady, $\mathcal{T}_s$=0 (e.g., holding arm upwards)

[4]Both global optimizers rely on multistart SQP-solvers, yet GO_1 integrates a scatter-search-based surrogate [22] with additional trial points.

[5]To better highlight the compromise in muscular performance $\|\boldsymbol{\alpha}\|$, the average from using random joints configurations is 4.41 ± 1.47.

to slow, regular (e.g., cutting), fast and swift execution, $\mathcal{T}_s$=1 (e.g., throwing a football). Similarly, $\mathcal{T}_i$ varies according to the task-intensity (acceleration/forces) and it is normalized from 0 to the maximum wrenches at maximum voluntary contraction (e.g., from experimental trials, we found 40 N for puncturing). Hence, we define $\mathcal{T}_i$=0 for negligible forces with a linear growth to the maximum $\mathcal{T}_i$=1. Finally, we defined $\mathcal{T}_r$ as a binary variable to assess repeatability of a task in terms of REBA (and RULA) ergonomics, i.e., if a task is repeated more than $4\times$ per minute. Notice the values for $\mathcal{T}_s, \mathcal{T}_i$, and $\mathcal{T}_r$ have been proposed based on heuristics and experience, yet they can be greatly improved with learning techniques and individual scalability.

To evaluate the efficiency of the manipulability representations for pHRC, we simulated the following scenarios.

1) Human-Robot Comfort-Based Handover: where Baxter grasps and positions a bottle/cup on a table for a human to grasp. We use $\mathcal{TS}$-comfortability to plan where to best position the bottle for human grasp in terms of comfortability, assuming a fixed position for the human and all possible power grasps around the bottle and normal to the palm. We simulated 100 scenarios with random values for the table placement, size, height and bottle height and weights (m). For design, we assumed half tasks were repetitive, e.g., a robot repeatably handing a bottle, and $\mathcal{T}_s$=0.5, $\mathcal{T}_i$=$m/30$.

2) Physical Human-Robot Cutting: depicts a collaborative application where the human uses a cutting tool to cut a board held by the two-arm robotic system. The goal is to plan the robot grasp that maximizes $\mathcal{TS}$-comfortability while satisfying kinematic and force constraints. For the 50 simulations, we varied the robot to human position, the cutting force and tool weight. We designed $\mathcal{T}_r$=0, $\mathcal{T}_s$=0.5, $\mathcal{T}_i$=$\|\boldsymbol{f}\|/40$, where $\boldsymbol{f}$ is the cutting force.

Results: for both tasks are shown in Table II depicting the average $\mathcal{TS}$-comfortability ϖ, MiTR $\underline{\omega_\alpha}$ and REBA values (lower the better) together with the computation time for the planner using the precomputed task-comfortability information. Table II also shows the comparison with three global-optimizer based planners—GO_1 Comf (max. (14)), Muscle-Only (8) and Ergo-only[6] (min. REBA r_e). Values are normalized by the results from the GO_1 Comf based planner.

As expected, an individual muscular-only based planner performs poorly when it comes to ergonomics. Similarly, an ergonomics-only based optimization leads to higher demands on muscular-activity. In contrast, both global-optimizer and pre-computed ϖ data based planners efficiently capture both aspects during pHRC tasks. This leads to improved $\mathcal{TS}$-comfortability ϖ results without compromising individual muscular-activity or ergonomics—which is one of the main motivations of this work.

Also, notice the usage of comfortability information leads to results close to GO_1 with considerable improvement in assessment time. For instance, taking the grasp-informed tabletop handover task, due to the efficient data structures an ϖ-based ordered set of human grasps with corresponding robot configurations can be retrieved $300\times$ faster when compared to GO_1 Comf. For the pHRC cutting, human configurations are retrieved in less than 1 s with most time spent on the generation of stable IK solutions for grasping.

[6]Ergonomics is optimized with a surrogate functions over the discrete values with additional multistart points to better address the stepwise REBA function, yet the use of a differentiable adaptation of REBA values, see e.g., [11], can lead to improved results in terms of time (same order of magnitude as the ones from the proposed method).

C. Human-Robot Experiments

Finally, we conducted a series of pHRC experiments to evaluate the efficiency of capturing and predicting possibly human actions by rapid queries on the $\mathcal{TS}$-comfortability distribution. To this aim, five participants[7] were asked to push a tool as hard as possible against a board held by the Baxter, simulating an elaborate peg-in-hole assembly, as shown in Fig. 5. Given the nature of the task, we captured the interaction between MiM and ErI with design parameters $\mathcal{T}_s$=0.5, $\mathcal{T}_i$=1 and $\mathcal{T}_r$=0. We measured the difference between the predicted and real values for the participant's muscle-, joint- and task-space configurations.[8] Fig. 5 illustrates one trial with possible poses to execute the task along the plane parallel to the prescribed force, as presented in the form of $\mathcal{TS}$-comfortability in side and top views.

Table III illustrates effectiveness of the proposed method. It leads to improved predictions and more consistent results when compared to purely muscular-informed or ergonomics assessment.[9] From predicted joint configurations, we also computed the predicted REBA score and the MiTR as shown in Table IV. Notably, a muscular-only approach focuses on maximizing MiTR in exchange of poor ergonomics, while the opposite happens with ergonomics-only. In practical applications, a combination of both better resembles human actions leading to a more accurate quality index for manipulation. Indeed, the average REBA and MiTR values computed from the experiments (3.2 ± 0.67 and 189.27 ± 44.99, respectively) were closer to $\mathcal{TS}$-comfortability.

Figure 5: The human-robot collaborative experiment is shown on the left, while figures on the right depict sections of the $\mathcal{TS}$-comfortability distribution around the plane of the board.

[7]Experiments were approved by University of Leeds' ethics committee (ID: MEEC 17-034) as per the Declaration of Helsinki. Participants profile: 24-37 years old, four males and one female (one left-hand dominant).

[8]Sensors were placed on 9 different anatomical positions covering main actuators (pectoralis m., ant. & post. delt., latiss. d., biceps b., lat. & med. triceps, and flexor & ext. carpi rad) for the corresponding motor task.

[9]The RMSE of the recorded muscles and estimated muscle-activity (from measured joints) is $.090 \pm .023$, that is only about 6% lower than the predicted muscle-activity from $\mathcal{TS}$-comfortability.

	Tabletop Handover			Time	pHRC Cutting			Time
	Comf. ϖ	MiTR $\underline{\omega_\alpha}$	REBA r_e		Comf. ϖ	MiTR $\underline{\omega_\alpha}$	REBA r_e	
GO_1- Comf	**1**	**1**	**1**	218.7 ± 43	**1**	1	1	353.7 ± 92
Muscle-Only	$.88 \pm .10$	$.93 \pm .11$	$1.23 \pm .28$	150.7 ± 51	$.87 \pm .32$	$.98 \pm .46$	$1.49 \pm .37$	256.8 ± 108
Ergo-Only	$.81 \pm .18$	$.61 \pm .27$	$1.06 \pm .25$	9.6 ± 0.26	$.72 \pm .25$	$.56 \pm .28$	$\mathbf{.98} \pm .27$	$21.1 \pm .18$
Comf. data	$.93 \pm .13$	$.85 \pm .24$	$1.07 \pm .25$	$\mathbf{0.673} \pm .05$	$.98 \pm .23$	$\mathbf{1.02} \pm .48$	$1.31 \pm .22$	$\mathbf{7.16} \pm 5.3$

Table II: Average $\mathcal{TS}$-comfortability and specific muscular-informed transmission rate (MiTR) and ergonomic (REBA) values for two different human-robot collaborative tasks (normalized with global optimizer GO_1- Comf results).

	Ergonomics-only	Muscular-Only	$\mathcal{TS}$-comfortability
$\boldsymbol{\alpha}_{\text{RMSE}}$	$.125 \pm .026$	$.113 \pm .030$	$\mathbf{.096} \pm .028$
$\|\boldsymbol{q}_e\|$	54.46 ± 15.14	51.20 ± 16.4	$\mathbf{43.70} \pm 14.8$
$\|\boldsymbol{p}_e\|$	10.45 ± 7.58	8.50 ± 4.07	$\mathbf{6.65} \pm 3.69$

Table III: Root-mean-square error from predicted normalized muscle-activity for 9 muscles and average joint-error norm $\|\boldsymbol{q}_e\|$ (in deg) and positioning $\|\boldsymbol{p}_e\|$ (in cm) compared to real experiments from 5 users performing 3 trials each.

	Ergonomics-only	Muscular-Only	$\mathcal{TS}$-comfortability
REBA	$2.67 \pm .49$	$3.87 \pm .64$	$2.93 \pm .46$
MiTR	168.05 ± 26.50	221.57 ± 36.08	194.89 ± 26.11

Table IV: Average REBA score (lower the better) and MiTR from predicted joint-configuration for all trials.

VI. Conclusion

We proposed a new method for predicting human comfort that combines two metrics: a muscle-activation-based metric and an ergonomy-based metric. This method brings together the advantages of the two metrics. We also proposed a voxelized data structure to precompute this metric, since online optimization can be too expensive for real-time operation.

Our experiments show that our combined metric can simultaneously optimize both ergonomy-based and muscle-activation-based comfort. They also show that interpolation using the voxelized data structure does not produce degraded comfort when compared with online optimization, while the latter is computationally extremely expensive. Experiments with real human subjects show that when presented with forceful robot-collaboration operations, they choose configurations that are consistent with our method's predictions.

Future directions for this work include integrating this metric into real-time planning and control of continuous human-robot collaboration tasks, and exploring the framework's inherent modularity to incorporate task-specific metrics, such as fatigue estimation, visibility and peripersonal-space comfort [2].

References

[1] L. M. Hiatt, C. Narber, E. Bekele, S. S. Khemlani, and J. G. Trafton, "Human modeling for human-robot collaboration," *International Journal of Robotics Research*, pp. 1–16, 2017.

[2] L. Chen, L. F. Figueredo, and M. R. Dogar, "Planning for muscular and peripersonal-space comfort during human-robot forceful collaboration," in *2018 IEEE-RAS 18th International Conference on Humanoid Robots (Humanoids)*, Nov 2018, pp. 1–8.

[3] L. Peternel, C. Fang, N. Tsagarakis, and A. Ajoudani, "Online human muscle force estimation for fatigue management in human-robot co-manipulation," in *2018 IEEE/RSJ International Conference on Intelligent Robots and Systems (IROS)*, 2018, pp. 1340–1346.

[4] D. Kulić, G. Venture, K. Yamane, E. Demircan, I. Mizuuchi, and K. Mombaur, "Anthropomorphic movement analysis and synthesis: A survey of methods and applications," *IEEE Transactions on Robotics*, vol. 32, no. 4, pp. 776–795, 2016.

[5] O. Khatib, E. Demircan, V. D. Sapio, L. Sentis, T. Besier, and S. Delp, "Robotics-based synthesis of human motion," *Journal of Physiology-Paris*, vol. 103, no. 3, pp. 211 – 219, 2009, neurorobotics.

[6] S. L. Delp, F. C. Anderson, A. S. Arnold, P. Loan, A. Habib, C. T. John, E. Guendelman, and D. G. Thelen, "Opensim: Open-source software to create and analyze dynamic simulations of movement," *IEEE Transactions on Biomedical Engineering*, vol. 54, no. 11, pp. 1940–1950, Nov 2007.

[7] K. R. Saul, X. Hu, C. M. Goehler, M. E. Vidt, M. Daly, A. Velisar, and W. M. Murray, "Benchmarking of dynamic simulation predictions in two software platforms using an upper limb musculoskeletal model Benchmarking of dynamic simulation predictions in two software platforms using an upper limb musculoskeletal model," *Computer Methods in Biomechanics and Biomedical Engineering*, vol. 18, no. 13, pp. 1445–1458, 2015.

[8] L. Peternel, C. Fang, N. Tsagarakis, and A. Ajoudani, "A selective muscle fatigue management approach to ergonomic human-robot co-manipulation," *Robotics and Computer–Integrated Manufacturing*, vol. 58, pp. 69–79, 2019.

[9] M. Lynn and N. Corlett, "RULA: A survey method for the investigation of work-related upper limb disorders," *Applied Ergonomics*, vol. 24, no. 2, pp. 91–99, 1993.

[10] L. McAtamney and S. Hignett, "Rapid Entire Body Assessment," *Handbook of Human Factors and Ergonomics Methods*, vol. 31, pp. 201–205, 2004.

[11] B. Busch, M. Toussaint, and M. Lopes, "Planning ergonomic sequences of actions in human-robot interaction," in *IEEE Int Conf Robot Automa (ICRA)*, May 2018, pp. 1916–1923.

[12] F. Zacharias, C. Borst, and G. Hirzinger, "Capturing robot workspace structure: representing robot capabilities," in *IEEE/RSJ International Conference on Intelligent Robots and Systems*, 2007, pp. 3229–3236.

[13] N. Vahrenkamp, E. Kuhn, T. Asfour, and R. Dillmann, "Planning multi-robot grasping motions," in *2010 10th IEEE-RAS International Conference on Humanoid Robots*, Dec 2010, pp. 593–600.

[14] F. E. Zajac, "Muscle coordination of movement: A perspective," *Journal of Biomechanics*, vol. 26, no. 1, pp. 109–124, 1993.

[15] D. Stanev and K. Moustakas, "Modeling musculoskeletal kinematic and dynamic redundancy using null space projection," *PLOS ONE*, vol. 14, no. 1, pp. 1–26, 01 2019.

[16] O. Khatib and J. Burdick, "Optimization of dynamics in manipulator design: The operational space formulation," *International Journal of Robotics and Automation*, vol. 2, no. 2, pp. 90–98, 1987.

[17] T. Yoshikawa, "Manipulability of robotic mechanisms," *The International Journal of Robotics Research*, vol. 4, no. 2, pp. 3–9, 1985.

[18] S. L. Chiu, "Task compatibility of manipulator postures," *The International Journal of Robotics Research*, vol. 7, no. 5, pp. 13–21, 1988.

[19] S. Patel and T. Sobh, "Manipulator performance measures - a comprehensive literature survey," *Journal of Intelligent & Robotic Systems*, vol. 77, no. 3, pp. 547–570, 2015.

[20] C. A. Klein and B. E. Blaho, "Dexterity measures for the design and control of kinematically redundant manipulators," *Int. J. Rob. Res.*, vol. 6, no. 2, pp. 72–83, Jul. 1987.

[21] W. Kim, M. Lorenzini, P. Balatti, P. D. H. Nguyen, U. Pattacini, V. Tikhanoff, L. Peternel, C. Fantacci, L. Natale, G. Metta, and A. Ajoudani, "Adaptable workstations for human-robot collaboration: A reconfigurable framework for improving worker ergonomics and productivity," *IEEE Robotics Automation Magazine*, vol. 26, no. 3, pp. 14–26, Sep. 2019.

[22] Z. Ugray, L. Lasdon, J. Plummer, F. Glover, J. Kelly, and R. Marti, "Scatter search and local NLP solvers: A multistart framework for global optimization," *INFORMS Journal Comput*, vol. 19, no. 3, 2007.